# DESIGN OF ORGANIC RANKINE CYCLE POWER SYSTEMS ACCOUNTING FOR EXPANDER PERFORMANCE

Angelo La Seta[1*], Jesper Graa Andreasen[2], Leonardo Pierobon[2], Giacomo Persico[3], Fredrik Haglind[2]

[1] Technical University of Denmark, Department of Mechanical Engineering,
2800 Kongens Lyngby, Denmark, and
Politecnico di Milano, Dipartimento di Energia,
20156 Milano, Italy
anlse@mek.dtu.dk
angelo.laseta@mail.polimi.it

[2] Technical University of Denmark, Department of Mechanical Engineering,
2800 Kongens Lyngby, Denmark
jgan@mek.dtu.dk, lpier@mek.dtu.dk, frh@mek.dtu.dk

[3] Politecnico di Milano, Dipartimento di Energia,
20156 Milano, Italy
giacomo.persico@polimi.it

* Corresponding Author

## ABSTRACT

Organic Rankine cycle power systems have recently emerged as promising solutions for waste heat recovery in low- and medium-size power plants. Their performance and economic feasibility strongly depend on the expander. Its design process and efficiency estimation are particularly challenging due to the peculiar physical properties of the working fluid and the gasdynamic phenomena occurring in the machine. Unlike steam Rankine and Brayton engines, organic Rankine cycle expanders have to deal with small enthalpy drops and large expansion ratios. These features yield turbine designs with few highly-loaded stages in supersonic flow regimes. This paper proposes a design method where the conventional cycle analysis is combined with calculations of the maximum expander performance using a validated mean-line design tool. The high computational cost of the turbine optimization is tackled building a model which gives the optimal preliminary design of the turbine as a function of the cycle conditions. This allows to estimate the optimal expander performance for each operating condition of interest. The test case is the preliminary design of an organic Rankine cycle turbogenerator to increase the overall energy efficiency of an offshore platform. The analysis of the results obtained using a constant turbine efficiency and the method proposed in this paper indicates a maximum reduction of the expander performance of 10 % – points for pressure ratios between 10 and 35. This work also demonstrates that this approach can support the plant designer on deciding the optimal size of the organic Rankine cycle unit when multiple exhaust gas streams are available.

## 1. INTRODUCTION

Environmental concerns stress the need for reducing greenhouse gas emissions and pollutants in the industrial, civil and transport sector. Organic Rankine cycle (ORC) power systems are an efficient and cost-competitive solution for heat-to-power conversion. These plants are nowadays regarded as a reliable technology for biomass and geothermal applications by virtue of the large operational experience. Current research efforts aim at enlarging their utilization range by progressing to the design of mini-ORC systems (3-20 kW) for challenging low heat source temperatures (90-150 °C) [6]. Concurrently,

ORC units are viable alternatives to steam Rankine cycle plants at high temperatures (300-500 °C), in niche sectors where the advantages of the ORC technology can be entirely exploited [5, 16].

In these applications, the turbine is arguably the most critical component owing to the small volumetric flow rates and the high expansion ratios [19]. The turbine performance tightly relates to the architecture of the thermodynamic cycle. Its design is of paramount importance for the technical and economic optimization of the power module. Numerous studies on the maximization of the cycle performance are available in the literature, see, e.g., [2, 17, 24, 26]. Few works address the feasibility of the turbine design, typically considered a posteriori or by setting bounds on the cycle parameters. As an example, Kang [14] selected the evaporation pressure of a 200 kW ORC unit with R245fa as working fluid considering a maximum expansion ratio of 4.11. Invernizzi et al. [13] employed the volumetric expansion ratio and the size parameter to identify a suitable working fluid for a bottoming mini-ORC unit. Astolfi et al. [3] performed a techno-economic optimization of a geothermal ORC power system. The cited authors estimated the number of turbine stages using information on the maximum volume flow ratio and the largest enthalpy drop.

The objective of this paper is to quantify how the variation of the expander efficiency influences the optimization of the thermodynamic cycle. A steady-state model of the thermodynamic cycle is coupled to a simulation tool capable of delivering the preliminary design of a single-stage turbine. This integration is performed optimizing the expander geometry for different boundary conditions of the cycle. A surrogate model of the turbine is then built to provide the maximum isentropic efficiency for each boundary condition. This approach gives a more realistic picture of the energy conversion efficiency of the system, when changing the key thermodynamic parameters of the cycle. The results are compared with those obtained assuming a constant isentropic turbine efficiency. This analysis demonstrates the impact of a proper modeling of the turbine for this class of power systems. The case study is the preliminary design of an ORC unit used to increase the overall energy efficiency of an offshore platform.

Section 2 presents the case study of this work. Section 3 describes the mean-line simulation tool for the design and optimization of the turbine. The results are then reported and discussed in Section 4. Concluding remarks are given in Section 5.

## 2. CASE STUDY

The case study is the power system installed on the Draugen oil and gas offshore platform, located 150 km from Kristiansund, in the Norwegian Sea. Three Siemens SGT-500 gas turbines are installed on the platform. The electrical power demand on board is 19 MW. Two turbines are kept in operation at all times, each covering 50 % of the load. The third is kept on stand-by, allowing for maintenance work. Despite the low energy conversion efficiency, this strategy ensures the necessary reserve power for peak loads and the safe operation of the engines.

The Siemens SGT-500 gas turbine is fed with natural gas and generates an electric power output of 16.5 MW. The mass flow rate and the temperature of the exhaust gases discharged by the engine are equal to 91.5 $kg \cdot s^{-1}$ and 625 K [24], respectively. The twin-spool engine employs two coaxial shafts coupling the low pressure compressor (LPC) with the low pressure turbine (LPT) and the high pressure compressor (HPC) with the high pressure turbine (HPT). The power turbine (PT) transfers mechanical power through a dedicated shaft to the electric generator (GEN). Recuperating the exhaust thermal power of the engines with an ORC unit may enhance their energy conversion efficiency. Figure 1 shows the layout of the power system, where one ORC unit is considered as bottoming unit for one gas turbine. The relatively low temperature of the exhaust gases enables to transfer the thermal energy directly to the once-through boiler (OTB), without the need for an intermediate oil loop. The working fluid first expands in the ORC turbine (TUR), and it is then cooled in the recuperator. In this way, the temperature of the organic compound at the OTB inlet may be increased by recovering energy from the superheated vapor exiting the turbine. The ORC fluid is then condensed and compressed to the highest pressure

level through the recuperator, thus closing the cycle. The selected organic compound is cyclopentane. According to the analysis performed by Pierobon et al. [24], this choice leads to the simultaneous optimization of net present value, plant efficiency and volume of the investigated ORC-unit. Moreover, this organic compound is already adopted for operating ORC systems in this range of temperature, see Del Turco et al. [10].

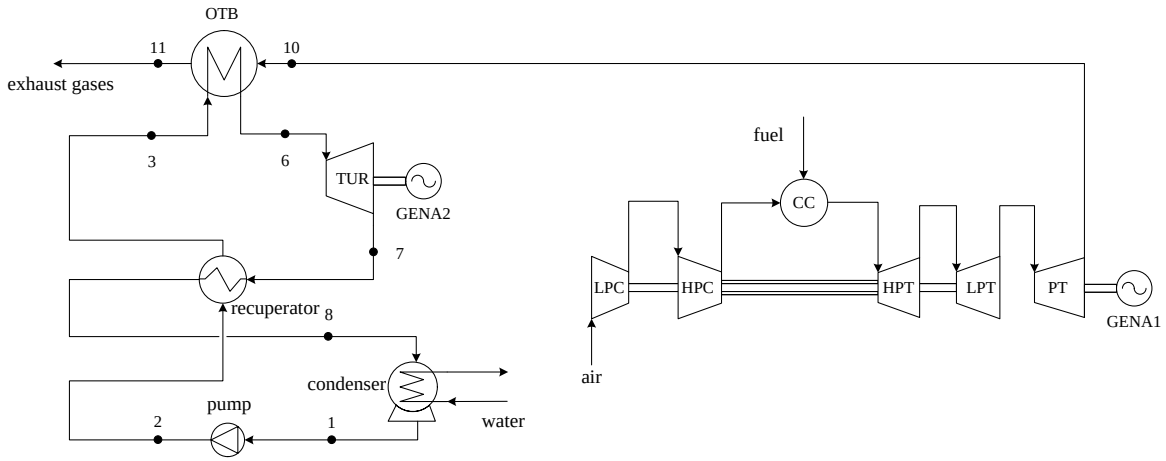


**Figure 1: Simplified layout of the power system on the Draugen offshore oil and gas platform; the exhaust gases of one engine feed the organic Rankine cycle module. The two remaining gas turbines are not shown.**

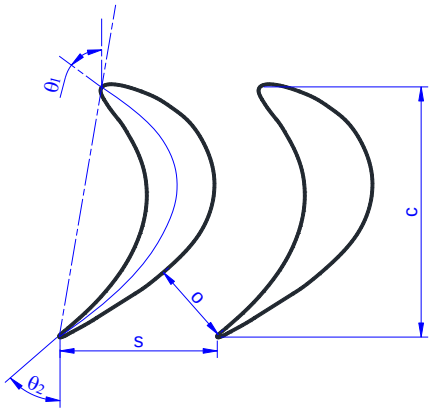


**Figure 2: Main geometric blade parameters with relative nomenclature.**

## 3. METHODS

### 3.1 The axial turbine simulation tool - TURAX

The large volume ratios and small enthalpy drops, commonly met in ORC turbines, entail higher volume flow ratios per stage compared to gas and steam turbines. The main problem is thus to distribute the load between stator and rotor in the most effective way. As discussed by Macchi [19], it is necessary to find a compromise between a pure impulse stage and a conventional configuration with a degree of reaction set to 0.5. The first one implies high Mach number of the relative velocity at the rotor inlet. Conversely, the latter demands large rotor blade height variations between inlet and outlet. A careful study is, therefore, necessary to find the optimal solution.

For the purpose of this work, a novel in-house code for turbine preliminary design, called TURAX, was written in the Matlab language. The simulation tool is the present result of ongoing development

at the Department of Mechanical Engineering, Technical University of Denmark, which began with a Master's Thesis work in 2013 [11]. For a given set of design parameters and boundary conditions, i.e., mass flow rate, inlet temperature, rotational speed and total pressure ratio, the simulation tool produces a preliminary design of a single- or multi-stage machine (see Figure 2 for the blade nomenclature) and an estimation of the total-to-total efficiency. Similarly to other preliminary design codes available in the literature, such as zTurbo [25], TURAX is based on one-dimensional approximation supported by proper correlations for the estimation of the losses and flow angles. The tool is combined with an external evolutionary algorithm to determine the optimal preliminary design.
The architecture of the code consists of three main parts:

1. Evaluation of the total inlet and total isentropic outlet thermodynamic states and of the total isentropic enthalpy drop. All these values remain constant during the design process.
2. Calculation of the set of first guess values for fluid angles, velocities and thermodynamic properties.
3. Iterative loop. Based on the first guess values, an iterative cycle runs until convergence is reached. The following steps are included in the iteration:
   (a) Calculation of the nozzle blade opening with the Deich formula [9]. If the flow is supersonic, this step allows to account for converging-diverging shapes of nozzle blades.
   (b) Evaluation of the blade and fluid angles. The blade angles $\theta_2$ and $\theta_3$ are obtained using the input parameters $(o/s)_{\mathrm{n}}$ and $(o/s)_{\mathrm{r}}$. The quantity $o/s$ is the outlet section-to-nozzle pitch ratio. The subscripts "n" and "r" refer to the nozzle and the rotor. For a subsonic case, the fluid angles are calculated with the equation proposed by Ainley and Mathieson [1]. The Vavra correlation is used for supersonic cases [29].
   (c) Updating of the fluid velocities with the calculated fluid angles and estimation of the thermodynamic properties and Mach numbers.
   (d) Calculation of the turbine geometry, e.g., flare angles, blade height, by means of the continuity equation.
   (e) Estimation of the turbine losses using the correlation proposed by Craig and Cox [7].
   (f) Calculation of the total-to-total turbine efficiency. Check the difference with respect to the previous iteration and return to step 3a until the relative deviation is smaller than $10^{-4}$.

The code is integrated with the optimization toolbox available in the Matlab language [28] to obtain the turbine layout which maximizes the total-to-total isentropic efficiency. The controlled elitist genetic algorithm, implemented as reported in Goldberg [12], is selected to find the optimal designs. Compared to gradient-based methods, a genetic algorithm is less prone to end its search in local minima of the problem and usually allows to converge towards global optima. This typically comes at the cost of an increased computational effort, due to the large number of the objective function evaluations [8]. Computational fluid dynamics tools tackle this issue by resorting to self-learning metamodels of the response surface [23]. However, in the present case the computational burden of a single evaluation is comparatively small, and it does not justify the use of metamodels. The genetic algorithm parameters are specified as follows: population size 900, generation size 200, crossover fraction 0.8, and migration fraction 0.2. These numerical values are selected to ensure the repeatability of the solution when different simulations are performed.

The vector of optimizing variables at hand reads

$$\bar{X} = [\psi, o_{\mathrm{n}}, o_{\mathrm{r}}, c_{\mathrm{n}}, c_{\mathrm{r}}, (o/s)_{\mathrm{n}}, (o/s)_{\mathrm{r}}, N] \,, \tag{1}$$

where $\psi$ is the stage work coefficient, and $N$ is the rotational speed of the machine, if considered among the optimization variable. The geometric variables $o$ and $c$ are the blade throat opening and the axial

chord. Note that the possible choice of seeking for a turbine geometry optimized for a certain rotational speed implies the insertion of a gearbox. The initialization of the optimizer requires to set the upper and lower bounds limiting the optimization variables. The Reynolds number for the blade opening, the ratio of the rotor height at the inlet to the nozzle height at the outlet as well as the Mach number for the converging/diverging nozzles are input parameters equal to $10^5$, 1.1 and 1.4, respectively. The axial velocity component is assumed constant throughout the stage. Additional constraints on the geometry and thermodynamic variables are necessary to provide acceptable solutions from physical and technological perspectives. These conditions, established by Macchi and Perdichizzi [20], are accordingly implemented as non-linear constraints. Table 1 lists the upper and lower bounds imposed on the dependent and independent variables.

The simulation tool is fully integrated with the freely-available high-accuracy property library for the estimation of the thermophysical properties of fluids developed by Bell et al. [4]. The fluid database uses Helmholtz-free-energy-based equations of state, provided in a temperature-density-explicit form, as source of thermodynamic data for many relevant working fluids [27]. The described fluid library offers two distinct interpolation methods: a) Tabular Taylor Series Expansion (TTSE) as outlined by Miyagawa and Hill [21] and Watanabe and Dooley [30], and b) bicubic interpolation reported in the work of Keys [15]. Bell et al. [4] provides a detailed description of these methods and of the benefits in terms of computational cost. The TTSE method is selected for the turbine optimization and the cycle calculations reported in this work.

**Table 1: Lower and upper bounds for the variables involved in the optimization of the turbine geometry. Additional constraints are also reported.**

| **Variable** | **Lower bound** | **Upper bound** |
|---|---|---|
| Stage work coefficient $\psi$ [-] | 2 | 6 |
| Blade throat opening $o$ [mm] | 2 | 100 |
| Axial chord $c$ [mm] | 10 | 100 |
| Outlet section-to-nozzle pitch $o/s$ [-] | 0.225 | 0.7 |
| Rotational speed (if optimized) [rpm] | 2000 | 12000 |
| **Additional constraints** | | |
| Relative Mach number at the rotor inlet [-] | 0 | 0.8 |
| Relative Mach number at the rotor outlet [-] | 0 | 1.4 |
| Number of blades (both for nozzle and rotor) [-] | 10 | 100 |
| Flare angles [°] | -25 | 25 |
| Blade height to mean diameter ratio [-] | 0.001 | 0.25 |
| Axial chord to mean diameter ratio [-] | 0 | 0.2 |

### 3.2 Model assessment

The software was verified using a similar code developed at the Politecnico di Milano [18]. Similarly to TURAX, this software can produce the optimal design of multiple stage axial-flow turbines. The code employs the same methods to estimate the fluid angles and the cascade losses. The test case for the comparison is the preliminary design of a single-stage axial machine for gas turbine applications. The expander rotates at 10 000 rpm with a mass flow rate of $10\,\mathrm{kg\cdot s^{-1}}$, a total turbine inlet temperature of 1123 K and an expansion ratio of 2. The comparison gives a relative error in isentropic efficiency lower than 0.2 %. Lower deviations are observed for most of the relevant geometric and flow variables. The relative error in the absolute fluid angle at rotor outlet is 0.5 %. This fluid angle is the highly sensible to the variations of the thermodynamic parameters. Given the relative errors reported above, the simulation tool is deemed reliable for preliminary design calculations.

### 3.3 Thermodynamic cycle calculation

The computation of the thermodynamic states is accomplished by applying the energy and mass balance equation to each plant constituent. This procedure yields the computation of the thermodynamic states at the inlet and outlet of each system component. Figure 3 illustrates the $T-s$ diagram for an ORC module with a turbine inlet pressure of 3 MPa, see Section 4. The nodes where the working fluid is in saturated conditions, i.e., 4, 5 and 9 in Figure 3, are not reported in the plant layout (Figure 1). The evaporation and condensation start inside the once-through boiler and the shell-and-tube condenser, respectively. A constant pressure specific heat capacity of $1100\,\mathrm{J\cdot kg^{-1}\cdot K^{-1}}$ is used for the energy balance calculations involving the exhaust gases. Note that this work considers only subcritical cycle configurations.

The condensing pressure is equal to 0.1 MPa to prevent air leakages into the engine. The pinch-point temperature differences of the once-through boiler and internal recuperator are fixed to 10 and 15 K, respectively. The pump isentropic efficiency and the electrical efficiency of the generator are equal to 0.8 and 0.98 [24]. Additional assumptions are the following: no pressure loss in piping or heat transfer equipment, adiabatic system, steady-state condition and homogeneous flow in terms of thermodynamic properties. Note that the turbine inlet temperature is kept at 513.15 K to ensure the chemical stability of the working fluid. The reader is referred to Pasetti et al. [22] for an in-depth analysis of the cyclopentane decomposition at high temperatures. A gearbox efficiency of 0.96 is used when the rotational speed is included in the turbine optimization.

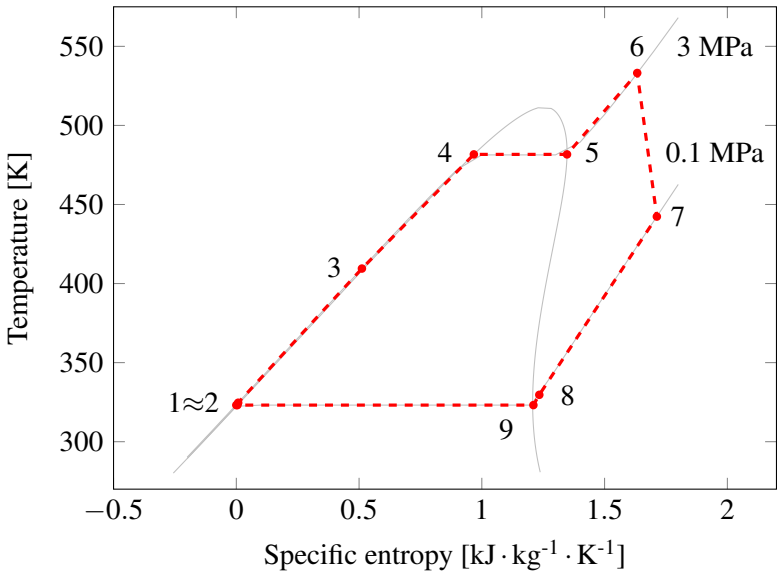


**Figure 3: Saturation curve of cyclopentane in a $T-s$ diagram, showing the thermodynamic cycle state points of the organic Rankine cycle system.**

## 4. RESULTS AND DISCUSSION

Figures 4 and 5 show the results for the turbine optimization at constant rotational speed (3000 rpm) and for the case where the rotational speed is optimized. The plots relate the total-to-total efficiency to the mass flow rate of the working fluid and the pressure ratio $\pi_e = p_{06}/p_{07}$. Each point in the figures represents a different optimal geometry obtained with a dedicated optimization. The efficiency curves initially increase, and, subsequently, flatten out. The results are in line with the trends reported by Macchi and Perdichizzi [20] for complex and monoatomic gases. As regarding the expender geometry, higher mass flow rates entail larger turbine sizes for the same pressure ratio. This results in wider blade channels and reduced relative influence of primary and secondary losses. Figure 6 shows an example of optimal geometry with relative velocity triangles. Removing the constraint on the rotational speed is extremely beneficial for the expander design. Figure 7 reports the optimal values obtained for this

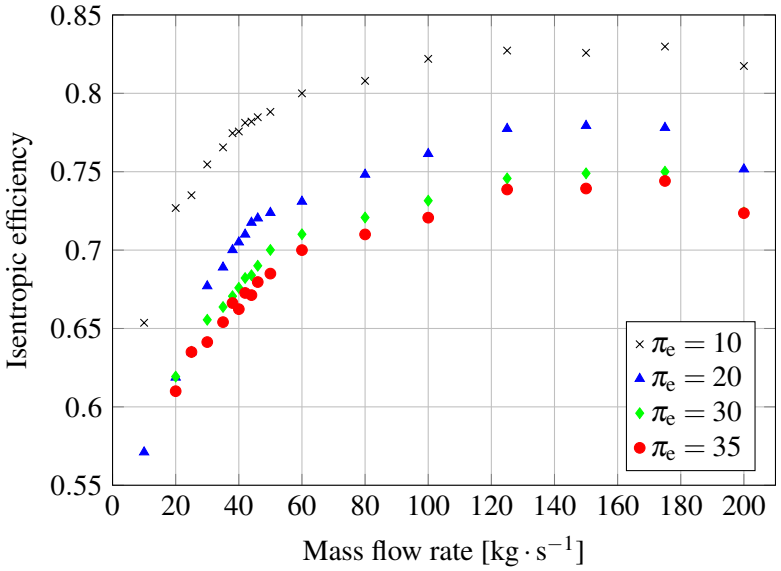


**Figure 4: Surrogate turbine model at fixed rotational speed. Total-to-total isentropic efficiency versus mass flow rate at different turbine pressure ratios.**

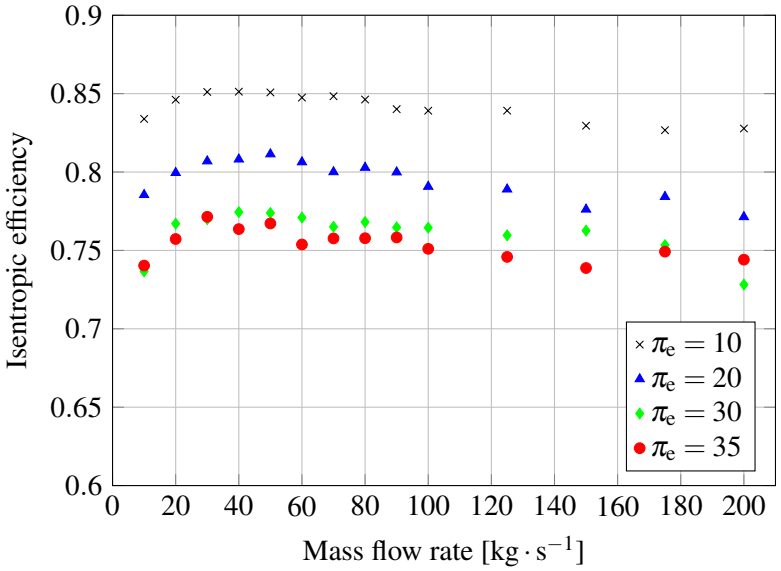


**Figure 5: Surrogate turbine model at the optimal rotational speeds. Total-to-total isentropic efficiency versus mass flow rate at different turbine pressure ratios.**

optimization variable. The highest gain in the turbine efficiency occurs at mass flow rates lower than 80 kg · s$^{-1}$. In this region, increasing the rotational speed allows for higher blade heights. Conversely, operating at constant rotational speed leads to an increment of the cascade losses for decreasing mass flow rates.

Figure 4 reports a maximum in efficiency around 120 kg · s$^{-1}$, while lower values are obtained for higher mass flow rates. This is caused by the increment of the profile losses in the nozzle. The rotor flare angle reaches the upper bound at around 120 kg · s$^{-1}$. At higher mass flow rates, the expansion across the stator and the axial velocity components increase. This results in higher losses and lower efficiency.

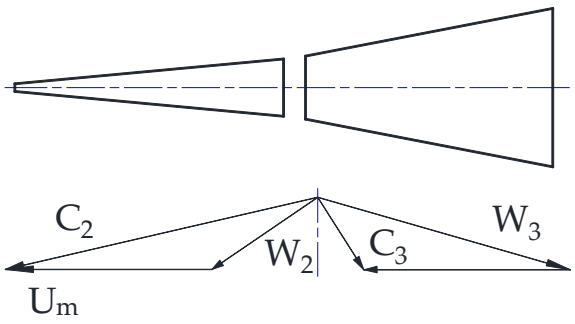


**Figure 6: The turbine section channel and relative velocity triangles at $\pi_e = 20$ and $38\,\mathrm{kg \cdot s^{-1}}$. The degree of reaction is 0.35.**

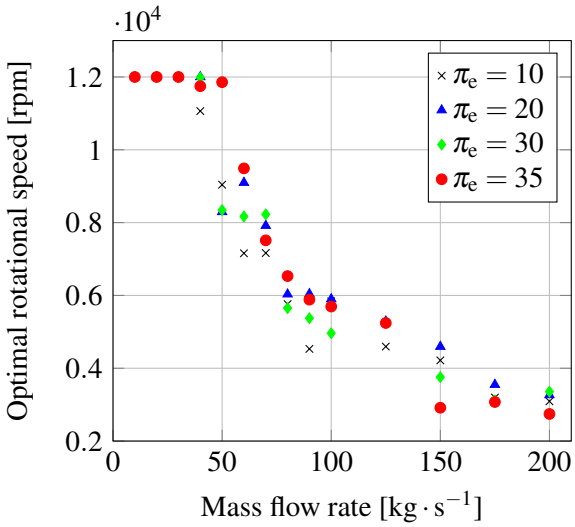


**Figure 7: Optimal rotational speed versus mass flow rate at different turbine pressure ratios for the second surrogate model.**

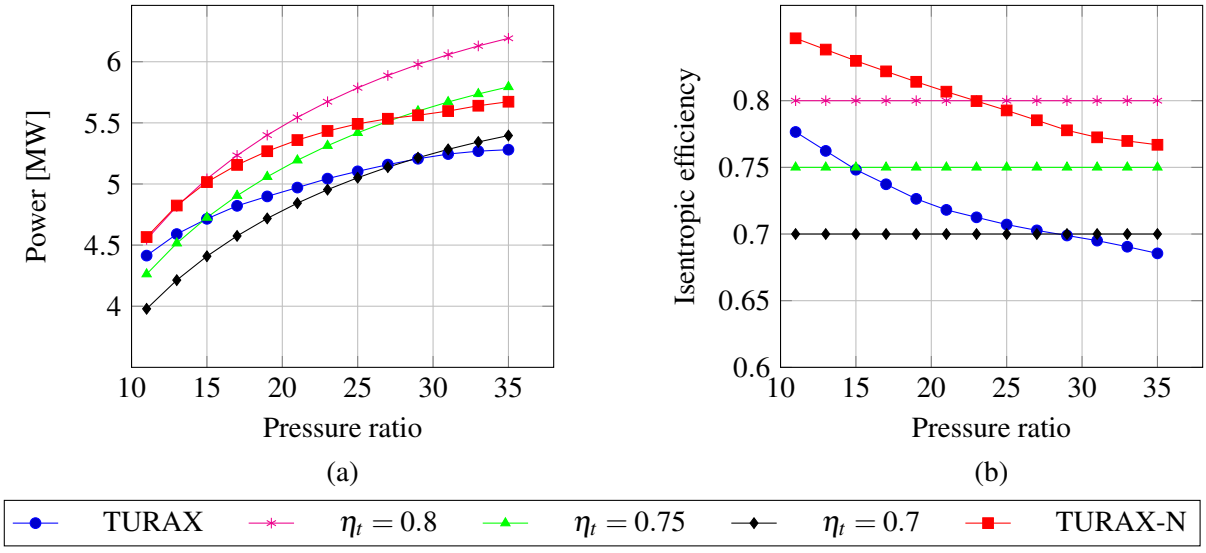


**Figure 8: Single exhaust gas configuration. 8(a) Net power output versus pressure ratio and 8(b) Total-to-total turbine isentropic efficiency versus pressure ratio.**

Figure 8a compares the ORC net power output at constant isentropic efficiency with that calculated using the turbine surrogate models. Given the assumptions reported in the previous section, the ratio $\pi_e$ is the only variable affecting the power output. The circulating mass flow rate varies between 45 and $50\,\mathrm{kg \cdot s^{-1}}$ for the reported range of $\pi_e$. The constant isentropic efficiency curves differ significantly compared to the trends observed with the surrogate models. This is owed to the progressive decrement of the expander performance at increasing pressure ratios, see Figure 8b. The computed isentropic efficiency decreases from 0.78 to 0.68 for the case with fixed rotational speed. The curve intersects the horizontal lines of constant efficiency. The intersections correspond to the values of pressure ratio for which the total-to-total efficiency coincides with the constant value. Accounting for the variability of the expander performance yields to a maximum difference in power output of 900 kW, compared to the results obtained assuming a fixed turbine efficiency of 80 %. This corresponds to a relative power decrement of 15 %.

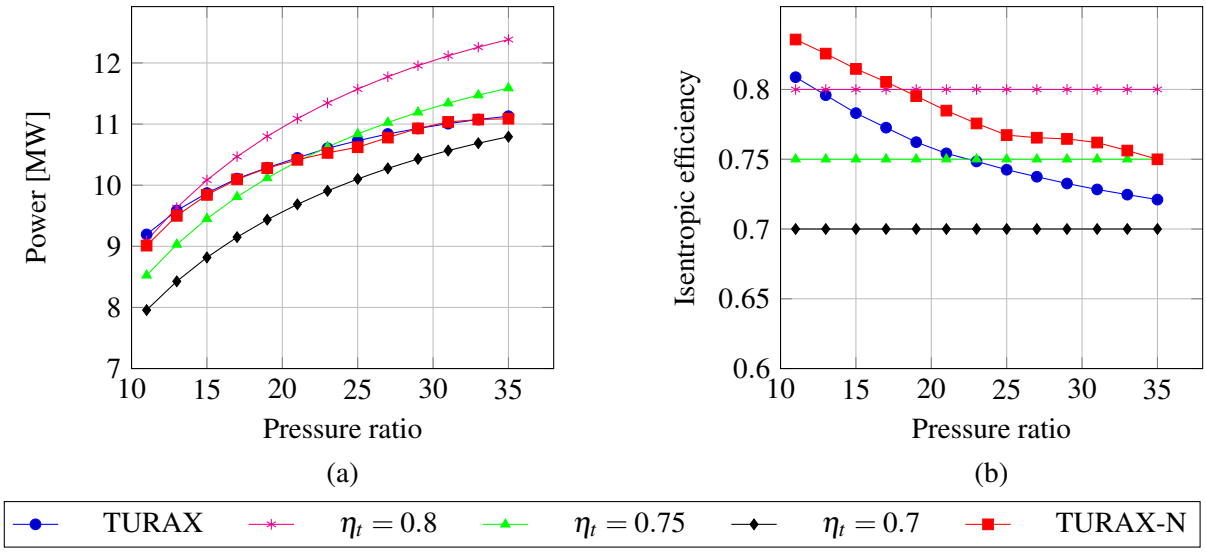


**Figure 9: Multiple exhaust gas configuration. 9(a) Net power output versus pressure ratio and 9(b) Total-to-total turbine isentropic efficiency versus pressure ratio.**

Figure 8b demonstrates that the optimization of the rotational speed increases averagely the expander efficiency of 8 %-points. The power curve is labeled as TURAX-N in Figures 8a and 8b. The improvement in power output is around 400 kW, corresponding to a relative increment of 7.4 %. This gain relates to the fact that the ORC unit operates in the range of mass flow rates where the expander efficiency is maximized. The highest power output occurs at the maximum available pressure ratio with just one stage, i.e., 35. Here the volumetric flow ratio reaches 43.5, a value close to the upper limit suggested by Macchi [19]. Further increments in the power output could be achieved by increasing the number of stages or adopting supercritical configurations. However, a larger number of stages implies higher investment costs. Moreover, the power curve in Figure 8b, obtained using the surrogate model, shows a progressively flattening trend for high values of pressure ratio. It is expected that the small power increments do not justify the technological (and economic) effort to operate at higher pressures. A complete techno-economic optimization should be carried out, in order to draw quantitative conclusions. However, such analysis is beyond the scopes of the current paper.

Figure 4 shows that the total-to-total isentropic efficiency of the turbine peaks at 120 $\mathrm{kg \cdot s^{-1}}$. This value is around three times the mass flow rate of the ORC unit fed by the exhaust gases of one gas turbine. Given that on the Draugen platform two engines operate at the same time, the opportunity of harvesting the heat from both energy sources with one ORC unit arises. This investigation assumes perfect mixing of the two exhaust gases. The engines are also equally sharing the load. As reported in Figure 9a, the trend of power versus pressure ratio is similar to that presented in the previous test. However, the power output obtained with the surrogate model is proportionally larger, being the values of turbine efficiency around 10 % higher. The integration of the ORC unit with one engine produces a net power of 5.3 MW. Conversely, the use of the exhaust heat of two gas turbines gives a total output of 11.1 MW. Therefore, the latter plant configuration offers a relative power increment of 5 %, compared to the implementation of two separate ORC turbogenerators. As shown in Figure 9b, the use of one ORC unit for two engines reduces the benefit of optimizing the rotational speed of the turbine. The increment in efficiency is smaller compared to the case of two separate ORC power systems. Moreover, Figure 9a shows that the mechanical losses of the gearbox partially overshadow the gain in turbine efficiency.

## 5. CONCLUSIONS

This paper documents the development of a simulation tool for the preliminary design of axial turbines. The model is integrated with a freely-available high-accuracy property library. This integration gives the possibility to minimize the computational time using advanced interpolation methods. The simulation tool is combined with the thermodynamic model of the ORC process in the form of a surrogate model giving the optimal turbine geometry at different boundary conditions. The method is applied to design an ORC power system for offshore applications.

The results obtained computing the expander performance using the surrogate model are compared with those assuming constant turbine isentropic efficiency. The power curves present different trends with a maximum relative discrepancy of 15 % in power output. The curve flattens at high turbine expansion ratios, if the expander design is taken into account. This trend arises doubts as to the benefit of increasing the design-point pressure ratio. The optimization of the rotational speed of the turbine improves the expander performance of 8 %-points, with a correspondent relative increment in power of 7.4 %. The power outputs of a single ORC turbogenerator recuperating the exhaust heat from two gas turbines are compared to the ones of one unit for each engine. The superior performance of larger scale expanders enables to achieve a 5 % improvement of power output using a single ORC power system. This latter configuration makes the implementation of a gearbox less attractive. The increased mechanical losses partially overshadow of the higher turbine isentropic efficiency.

## NOMENCLATURE

| | |
|---|---|
| $C$ | absolute fluid velocity [$m \cdot s^{-1}$] |
| $N$ | rotational speed [rpm] |
| $U$ | peripheral velocity [$m \cdot s^{-1}$] |
| $W$ | relative fluid velocity [$m \cdot s^{-1}$] |
| $\bar{X}$ | array of the optimizing variables |
| $c$ | axial chord [m] |
| $o$ | blade throat opening [m] |
| $p$ | pressure [Pa] |
| $s$ | blade pitch [m] |

**Abbreviations and acronyms**

| | |
|---|---|
| CC | combustion chamber |
| GEN | electric generator |
| HPC | high pressure compressor |
| HPT | high pressure turbine |
| LPC | low pressure compressor |
| LPT | low pressure turbine |
| ORC | organic Rankine cycle |
| OTB | once-through boiler |
| PT | power turbine |
| TUR | organic Rankine cycle expander |

**Greek letters**

| | |
|---|---|
| $\eta_{is,t}$ | turbine isentropic efficiency |
| $\pi_e$ | pressure ratio |
| $\psi$ | stage loading coefficient |
| $\theta$ | blade angle [°] |

**Subscripts**

| | |
|---|---|
| 2 | rotor inlet |
| 3 | rotor outlet |
| m | referred to average diameter |
| n | nozzle |
| r | rotor |

## REFERENCES

[1] Ainley, D. and Mathieson, G. (1951). An examination of the flow and pressure losses in blade rows of axial-flow turbines. Technical report, Ministry of Supply - Aeronautical Research Council.

[2] Andreasen, J. G., Larsen, U., Knudsen, T., Pierobon, L., and Haglind, F. (2014). Selection and optimization of pure and mixed working fluids for low grade heat utilization using organic Rankine cycles. *Energy*, 73:204–213.

[3] Astolfi, M., Romano, M. C., Bombarda, P., and Macchi, E. (2014). Binary ORC (Organic Rankine Cycles) power plants for the exploitation of medium low temperature geothermal sources - Part B: Techno-economic optimization. *Energy*, 66:435–446.

[4] Bell, I. H., Wronski, J., Quoilin, S., and Lemort, V. (2014). Pure and pseudo-pure fluid thermophysical property evaluation and the open-source thermophysical property library CoolProp. *Industrial & Engineering Chemistry Research*, 53(6):2498–2508.

[5] Casati, E., Galli, A., and Colonna, P. (2013). Thermal energy storage for solar-powered organic Rankine cycle engines. *Solar energy*, 96:205–219.

[6] Colonna, P. (2012). Developments from the early days, current status and an outlook on relevant research topics and new applications. In *Proceedings of International Symposium on Advanced Waste Heat Valorisation Technologies*, Kortrijk, Belgium.

[7] Craig, H. and Cox, H. (1970). Performance estimation of axial flow turbines. *Proceedings of the Institution of Mechanical Engineers*, 185(1):407–424.

[8] Deb, K. (2001). *Multi-objective optimization using evolutionary algorithms*. John Wiley & Sons, Inc., West Sussex, Great Britain.

[9] Deich, M., Filippov, G., and Lazarev, L. (1965). *Atlas of Axial Turbine Blade Cascades*. C.E. Trans. 4563-4564. CEGB Information Services.

[10] Del Turco, P., Asti, A., Del Greco, A., Bacci, A., Landi, G., and Seghi, G. (2011). The ORegen waste heat recovery cycle: Reducing the $CO_2$ footprint by means of overall cycle efficiency improvement. In *ASME Turbo Expo 2011*, pages 547–556, Vancouver, Canada.

[11] Gabrielli, P. (2014). Design and optimization of turbo-expanders for organic rankine cycles. Master's thesis, Technical University of Denmark.

[12] Goldberg, D. E. (1989). *Genetic Algorithms in Search, Optimization and Machine Learning*. Addison-Wesley Longman Publishing Co., Inc., Boston, MA, USA, 1st edition.

[13] Invernizzi, C., Iora, P., and Silva, P. (2007). Bottoming micro-Rankine cycles for micro-gas turbines. *Applied Thermal Engineering*, 27(1):100–110.

[14] Kang, S. H. (2012). Design and experimental study of ORC (organic Rankine cycle) and radial turbine using R245fa working fluid. *Energy*, 41(1):514–524.

[15] Keys, R. G. (1981). Cubic convolution interpolation for digital image processing. *IEEE Proceedings. Nanobiotechnology Transactions On Acoustics, Speech, And Signal Processing*, 29(6):1153–1160.

[16] Lang, W., Colonna, P., and Almbauer, R. (2013). Assessment of waste heat recovery from a heavy-duty truck engine by means of an ORC turbogenerator. *Journal of Engineering for Gas Turbines and Power*, 135(4):1–10.

[17] Larsen, U., Pierobon, L., Haglind, F., and Gabrielii, C. (2013). Design and optimisation of organic Rankine cycles for waste heat recovery in marine applications using the principles of natural selection. *Energy*, 55(0):803 – 812.

[18] Lozza, G., Macchi, E., and Perdichizzi, A. (1982). On the influence of the number of stages on the efficiency of axial-flow turbines. In *American Society of Mechanical Engineers, International Gas Turbine Conference and Exhibit, 27th*, London, England.

[19] Macchi, E. (1977). Design criteria for turbines operating with fluids having a low speed of sound. *Von Karman Institute for Fluid Dynamics*, 2:1–64.

[20] Macchi, E. and Perdichizzi, A. (1981). Efficiency prediction for axial-flow turbines operating with nonconventional fluids. *Journal of Engineering for Gas Turbine and Power*, 103(4):718–724.

[21] Miyagawa, K. and Hill, P. G. (2001). Rapid and accurate calculation of water and steam properties using the tabular taylor series expansion method. *Journal of Engineering for Gas Turbines and Power*, 123(3):707–712.

[22] Pasetti, M., Invernizzi, C. M., and Iora, P. (2014). Thermal stability of working fluids for organic Rankine cycles: An improved survey method and experimental results for cyclopentane, isopentane and n-butane. *Applied Thermal Engineering*, 73(1):762 – 772.

[23] Pasquale, D., Persico, G., and Rebay, S. (2013). Optimization of turbomachinery flow surfaces applying a CFD-based throughow method. *Journal of Turbomachinery*, 136(3):1–11.

[24] Pierobon, L., Nguyen, T.-V., Larsen, U., Haglind, F., and Elmegaard, B. (2013). Multi-objective optimization of organic Rankine cycles for waste heat recovery: Application in an offshore platform. *Energy*, 58(0):538–549.

[25] Pini, M., Persico, G., Casati, E., and Dossena, V. (2013). Preliminary design of a centrifugal turbine for organic rankine cycles applications. *Journal of Engineering for Gas Turbine and Power*, 135(4):1–9.

[26] Quoilin, S., Orosz, M., Hemond, H., and Lemort, V. (2011). Performance and design optimization of a low-cost solar organic Rankine cycle for remote power generation. *Solar Energy*, 85(5):955–966.

[27] Span, R., Wagner, W., Lemmon, E. W., and Jacobsen, R. T. (2001). Multiparameter equations of state—recent trends and future challenges. *Fluid Phase Equilibria*, 183:1–20.

[28] The MathWorks, Inc. (2014). *Optimization Toolbox™ User's Guide*. The MathWorks, Inc., Natick, Massachusetts.

[29] Vavra, M. H. (1969). Axial flow turbines. *Von Karman Institute for Fluid Dynamics*, 15.

[30] Watanabe, K. and Dooley, R. B. (2003). Guideline on the Tabular Taylor Series Expansion (TTSE) Method for Calculation of Thermodynamic Properties of Water and Steam Applied to IAPWS-95 as an Example. Technical report, The International Association for the Properties of Water and Steam, Vejle, Denmark.